Long room-temperature electron spin lifetimes in bulk cubic GaN

J. H. Buß,[a] J. Rudolph,[a] T. Schupp,[b] D. J. As,[b] K. Lischka,[b] and D. Hägele[a]

[a]Arbeitsgruppe Spektroskopie der kondensierten Materie, Ruhr-Universität Bochum, 44801 Bochum, Germany;
[b]Department of Physics, University of Paderborn, Warburger Str. 100, 33098 Paderborn, Germany

ABSTRACT

We report on very long electron spin lifetimes in cubic GaN measured by time-resolved Kerr-rotation-spectroscopy. The spin coherence times with and without external magnetic field exceed 500 ps at room temperature, despite a high n-type doping level of more than 10^{19} cm^{-3} in the bulk sample under investigation. Our findings are therefore highly relevant for spin optoelectronics in the blue wavelength regime. The spin lifetimes are found to be almost temperature independent in accord with a prediction for degenerate electron gases of Dyakonov and Perel from 1972. These results are discussed also in comparison to wurtzite GaN, which shows much shorter spin lifetimes and a dependence of spin lifetimes on the spin orientation.

Keywords: spin relaxation, zincblende and wurtzite bulk GaN

1. INTRODUCTION

The idea to incorporate the electron's spin degree of freedom into semiconductor-based electronics has stimulated intense research in the field of so-called spintronics.[1] Some of the basic requirements for a successful implementation of spintronics concepts are the alignment of electron spins for spin injection as well as slow spin relaxation for electron spin transport and storage. Against this background, the wide-gap semiconductor GaN has attracted growing interest, as it has been predicted to show above room-temperature ferromagnetism upon doping with rare-earth atoms[2] and as it shows a comparably small spin-orbit coupling which should result in slow spin relaxation. Its good optical properties make it also highly promising for spin-optoelectronics[3] in the blue to ultraviolet spectral region.[4] The thermodynamically stable wurtzite phase of GaN shows, however, only short spin relaxation times, which can be explained by the comparably low symmetry of its hexagonal structure.[5,6] The metastable zincblende (ZB) phase of GaN circumvents this limitation due to its higher cubic symmetry, promising slow spin relaxation.[7,8] Long spin relaxation times are especially hard to realize in highly n-doped semiconductors,[9] which are nonetheless required for, e.g., contact layers. Here, we use time-resolved Kerr-rotation (TRKR) measurements to investigate electron spin relaxation in highly n-doped bulk cubic GaN. The long spin relaxation times exceeding 500 ps up to room-temperature despite the high doping level of more than 10^{19} cm^{-3} demonstrate the materials large potential for spintronics.

2. SAMPLES AND TIME-RESOLVED KERR-ROTATION MEASUREMENTS

The bulk cubic GaN (001) samples investigated were grown by plasma assisted molecular beam epitaxy.[10] First, a 30 nm-thick ZB-AlN (001) barrier was deposited pseudomorphically strained on the 3C-SiC (001) substrate[11] to avoid carrier escape to the substrate. The top 570 nm-thick ZB-GaN layer was n-type doped by Si evaporated from a standard effusion cell. The wurtzite phase content of a sample grown under optimal conditions (sample A) was determined by high resolution x-ray diffraction (HRXRD) measurements to be less than the HRXRD detection limit of 0.3%. A second sample (sample B) was grown under suboptimal conditions, resulting in a wurtzite phase content $\leq$ 2.5% as determined by HRXRD. Capacitance-Voltage measurements showed a net

Further author information: (Send correspondence to J. H. Buß)
J. H. Buß: E-mail: jan.buss@ruhr-uni-bochum.de, Telephone: 0049-234-32-23576

carrier concentration $n = (1.0\ +1.0/-0.5) \times 10^{19}$ cm^{-3} at room-temperature. The samples were kept in a cold-finger cryostat at temperatures between 22 K and 300 K. For the TRKR measurements, frequency-doubled femtosecond pump and probe pulses were derived from a mode-locked Ti:sapphire laser with a repetition rate of 80 MHz. The energy of both beams was varied between 3.29 eV and 3.24 eV to follow the temperature induced decrease of the band gap at higher temperatures. The polarization of the pump beam was modulated between right and left circularly polarized, respectively, by a photo-elastic modulator at 50 kHz. The pump beam was focused down to a spot of about 60 μm diameter on the sample surface to create a spin-polarized electron ensemble. The spin dynamics was monitored via the Kerr-effect of the linearly polarized probe pulse that was time delayed by a variable mechanical delay-line and modulated by a mechanical chopper at a frequency of ≈ 1.2 kHz. A cascaded lock-in amplifier technique was used, where the output of a first lock-in amplifier, which was locked to the polarization modulation of the pump beam, was fed into a second lock-in amplifier locked to the modulation of the probe beam. The average power of pump and probe beam was kept at 10 mW and 1 mW, respectively, which corresponds to an estimated density of $n_{\rm exc} = 5 \times 10^{16}$ cm^{-3} of photo-excited carriers. An external magnetic field $B_{\rm ext}$ was applied in the sample plane.

3. RESULTS AND DISCUSSION

Typical TRKR transients are shown in Figure 1(a) for sample A and B at a temperature $T = 80$ K and in an external magnetic field $B_{\rm ext} = 270$ mT. The temporal oscillation of the TRKR signal is caused by Larmor precession of the electron spins around the external magnetic field. The temporal decay of the TRKR amplitude is generally due to the decay of the carrier density as well as of the electron spin polarization. Time-resolved reflectivity (TRR) measurements showed, however, a fast decay of the carrier density [cf. Fig. 1(b)] with a decay time $\tau_c \approx 50$ ps. The decay of the TRKR signal at times $t \gg 50$ ps is therefore solely due to the decreasing electron spin polarization caused by spin relaxation. The corresponding spin relaxation time τ_s was determined by damped-cosine fits of the form $[A_1 \exp(-t/\tau_c) + A_2] \exp(-t/\tau_s) \cos[\omega_L(t - t_0)]$ to the TRKR transients for $B_{\rm ext} > 0$ and by exponential decay fits $[A_1 \exp(-t/\tau_c) + A_2] \exp(-t/\tau_s)$ to the zero-field transients.

In the following, we will concentrate on sample A (high phase purity). First, the dependence of the spin relaxation time τ_s on the energy $E_{\rm L}$ of pump and probe beam was investigated (cf. Figure 2(a) for $T = 80$ K). The laser energies $E_{\rm L} = 3.27$ eV to 3.34 eV are centered at the high-energy edge of the broad, strongly asymmetric photoluminescence spectrum (not shown), being typical for heavily n-doped bulk semiconductors.[12] The spin relaxation time shows in this energy range no dependence on $E_{\rm L}$. A laser energy $E_{\rm L} = 3.29$ eV was chosen at $T = 80$ K in the following, where the TRKR signal amplitude was highest. The laser energy was adapted according to the Varshni relation for other temperatures to account for the temperature induced shift of the bandgap E_g. Next, the dependence of spin relaxation on the power $P_{\rm pump}$ of the pump beam was checked with a fixed ratio of 10:1 between pump and probe power. For pump powers $P_{\rm pump} = 1.8$ mW to 11.3 mW, corresponding to an estimated photo-excited carrier density $n_{\rm exc} = 9 \times 10^{15}$ cm^{-3} to 5.7×10^{16} cm^{-3}, the spin relaxation time is constant, as is expected for the much higher doping concentration $n_D = 2 \times 10^{19}$ cm$^{-3} \gg n_{\rm exc}$. The pump power is kept at $P_{\rm pump} = 10$ mW in the following.

As the central result, we will now discuss the temperature dependence of spin relaxation.[13] Figure 3(a) shows the spin relaxation time τ_s for temperatures from 22 K to 295 K. The temperature dependence of τ_s exhibits two remarkable features: First, the spin relaxation time τ_s is almost independent of the temperature, as can also already be seen from the almost identical slope of the TRKR transients in the semi-log plot in Figure 1(c). A second striking feature is the very long spin relaxation time, which still exceed 500 ps at room-temperature despite the very high doping level, whereas spin relaxation times in GaAs are almost two orders of magnitude shorter at the same doping level.[9] In the following, we will show that both characteristics can be well explained by Dyakonov-Perel spin relaxation theory[14] for the highly degenerate regime. Dyakonov-Perel electron spin relaxation follows from an intrinsic conduction band spin-splitting, which is caused by spin-orbit coupling. This spin-splitting is described by a Hamiltonian of the form $H_{so} = (\hbar/2)\mathbf{\Omega}(\mathbf{k}) \cdot \boldsymbol{\sigma}$ with $\boldsymbol{\sigma}$ as the vector of Pauli spin matrices. In analogy to the Zeeman effect, $\mathbf{\Omega}(\mathbf{k})$ is easily interpreted as an effective magnetic field, which acts on the electron spins and depends on the electron wavevector $\mathbf{k}$. Random changes of the wavevector $\mathbf{k}$ due to scattering cause a randomly fluctuating effective magnetic field $\mathbf{\Omega}(\mathbf{k})$ around which the electron spins precess,

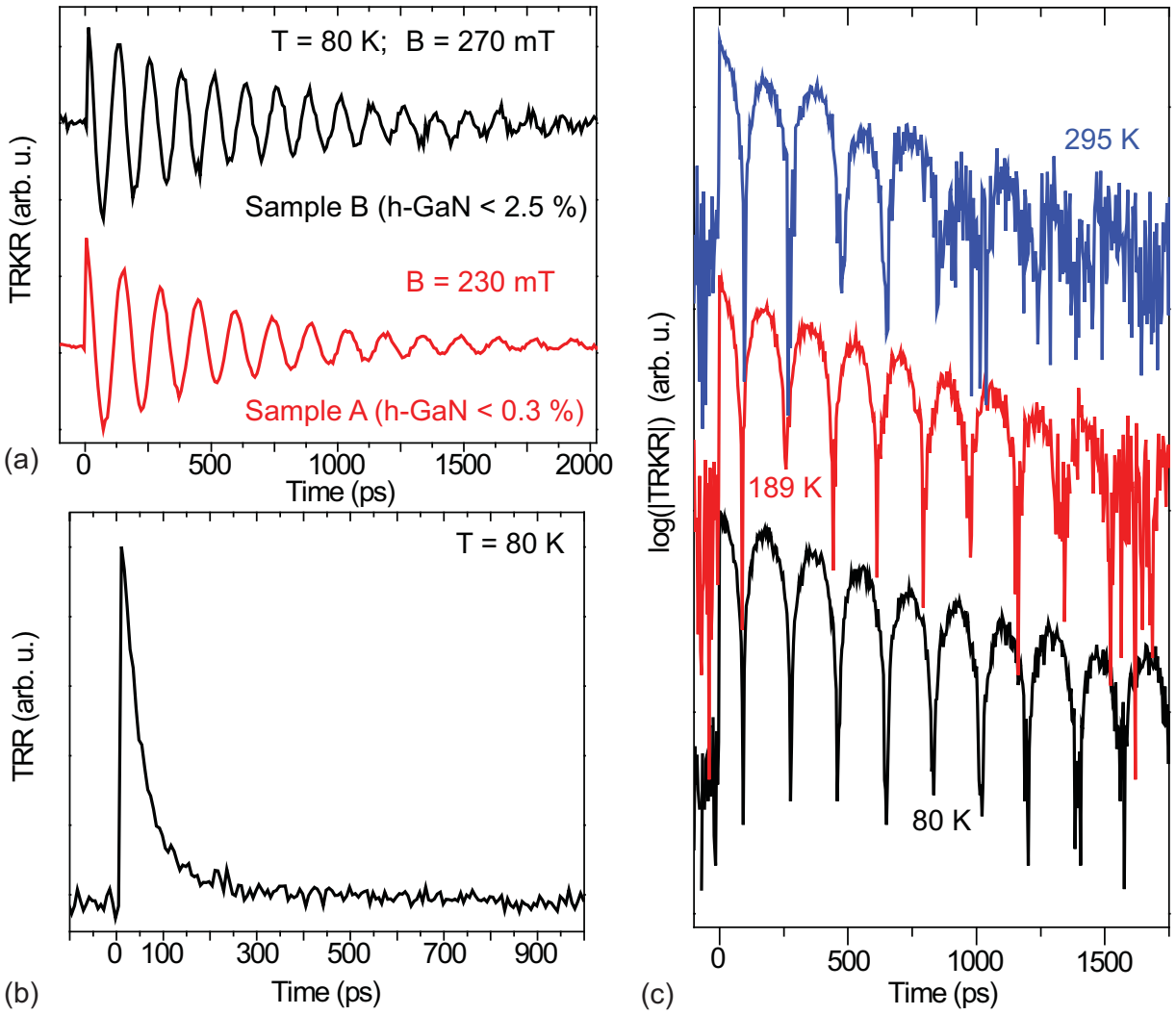

Figure 1. (a) TRKR transients for sample A with small wurtzite phase content $< 0.3\%$ and sample B with higher wurtzite phase content $\leq 2.5\%$ at $T = 80$ K and in an external magnetic field $B_{\rm ext} = 270$ mT and 230 mT, respectively. (b) Time-resolved reflectivity transient for sample A, demonstrating the rapid decay of the carrier concentration with a decay time $\tau_c \approx 50$ ps. (c) Semi-log plot of the absolute values of the TRKR transients for sample A at temperatures $T = 80$ K, 189 K and 295 K in an external magnetic field $B_{\rm ext} = 110$ mT.

leading finally to spin relaxation for an ensemble of electron spins. The intrinsic spin-splitting is in zincblende semiconductors given by the Dresselhaus term[15]

$$H_{so} = \Gamma_e \sum_i \sigma_i k_i (k_{i+1}^2 - k_{i+2}^2) \ ,$$

where $i = x, y, z$ are the principal crystal axes with $i + 3 \rightarrow i$, σ_i are the Pauli spin matrices and Γ_e is the spin-splitting constant. The effective magnetic field is correspondingly given by $\Omega_i(\mathbf{k}) = (2\Gamma_e/\hbar) k_i (k_{i+1}^2 - k_{i+2}^2)$. A spin relaxation rate

$$\gamma_{ij}(k) = \left(\delta_{ij} \langle \mathbf{\Omega}^2 \rangle_{\phi,\theta} - \langle \Omega_i \Omega_j \rangle_{\phi,\theta} \right) \tau_p \qquad (1)$$

follows in the most simplistic form of Dyakonov-Perel theory, where $\langle \ldots \rangle_{\phi,\theta}$ denotes averaging over the directions of $\mathbf{k}$ and τ_p is the momentum scattering time. The spin relaxation rate in cubic bulk material is a scalar quantity,

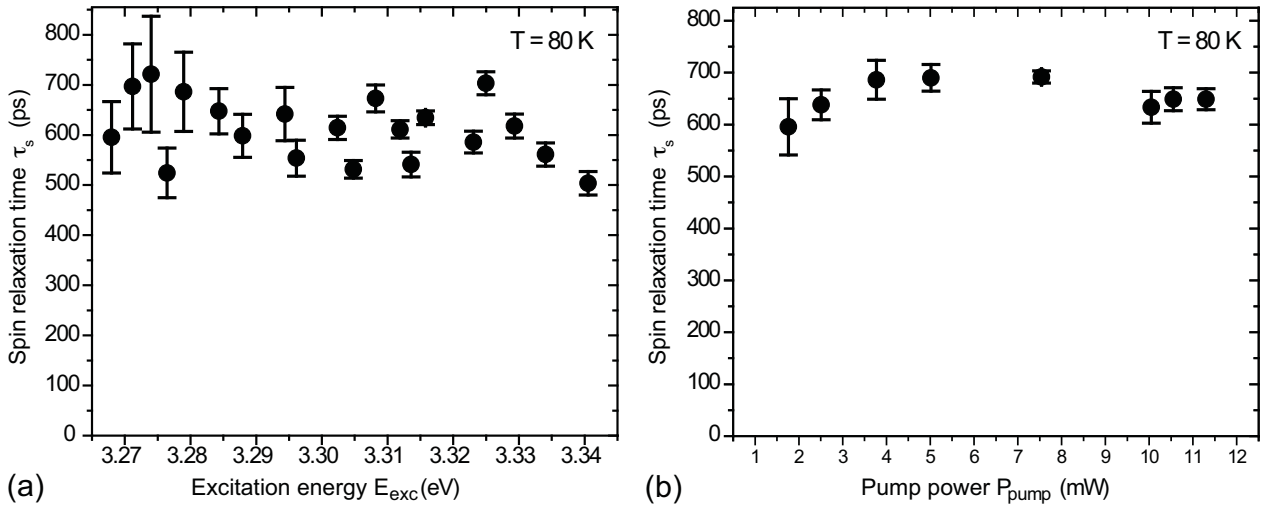

Figure 2. (a) Spin relaxation time τ_s in dependence of the laser energy E_L for sample A at a temperature of $T = 80$ K. (b) Pump power dependence of the spin relaxation time for sample A at $T = 80$ K.

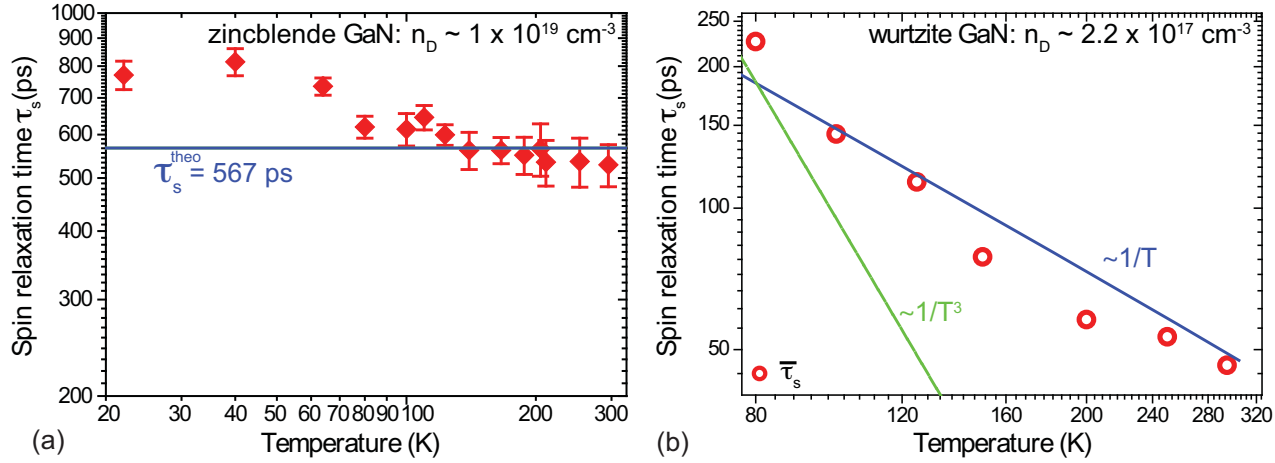

Figure 3. (a) Temperature dependence of the spin relaxation time τ_s for sample A. The solid blue line indicates the spin relaxation time calculated by Dyakonov-Perel theory for the degenerate regime. (b) Temperature dependence of the spin relaxation time τ_s in a moderately n-doped bulk wurtzite GaN sample. The solid blue line is the prediction of Dyakonov-Perel theory for spin relaxation due to a k-linear spin splitting, the dashed green line shows a hypothetical decrease due to a k^3-dependent spin splitting.

which follows from Eqn. (1) as

$$\gamma(k) = \frac{32}{105}\frac{\Gamma_e k^6}{\hbar^2}\tau_p \ .$$

The spin relaxation time $\tau_s = 1/\langle\gamma(k)\rangle_k$ is obtained by averaging over the electron momentum distribution. For a non-degenerate electron gas, a Boltzmann momentum distribution can be assumed and a spin relaxation time $\tau_s^{non} \propto 1/T^3$ follows. In a highly degenerate electron gas, in contrast, k corresponds to the Fermi wavevector k_F and a spin relaxation time

$$\tau_s = \frac{105}{256}\frac{\hbar^8}{\Gamma_e^2 E_F^3 m^{*3}}\frac{1}{\tau_p} \tag{2}$$

follows using the Fermi energy $E_F = (3\pi^2)^{2/3}\hbar^2 n_D^{2/3}/2m^*$. The momentum scattering time τ_p is expected to be governed by electron-impurity scattering in the degenerate regime, for which a temperature-independent

scattering time ($\tau_p(T) = const.$) follows in the Brooks-Herring formalism.[1] The spin relaxation time τ_s in the degenerate regime is therefore almost temperature-independent. The high doping level $n_D = 2 \times 10^{19}$ cm^{-3} of the investigated sample corresponds to a Fermi temperature $T_F = E_F/k_B \approx 1100$ K, which is well above the lattice temperature for the whole temperature range of the measurements. The sample is therefore for all investigated temperatures in the highly degenerate regime and the observed very weak temperature dependence is in good agreement with the prediction of Dyakonov-Perel theory.

The magnitude of the spin relaxation time is primarily determined by the spin-splitting constant Γ_e. As a general tendency, spin-orbit coupling effects can be expected to be the smaller the lighter the constituent atoms of a semiconductor are. From this point of view, a smaller value of Γ_e is expected for GaN than for, e.g., GaAs. The symmetry of the crystal lattice plays, however, also an important role as is highlighted by the comparison of the wurtzite and zincblende phase of GaN. Figure 3(b) shows the temperature dependence[5] of the spin relaxation time τ_s for a moderately n-doped bulk wurtzite GaN sample on a double-logarithmic scale. The spin relaxation time follows clearly a $\tau_s \propto T^{-1}$ powerlaw instead of the $\tau_s \propto T^{-3}$ powerlaw predicted by the Dresselhaus term that also exists in the wurtzite structure. The $\tau_s \propto T^{-1}$ behavior proves that spin relaxation in the wurtzite phase of GaN is dominated by a k-linear contribution to the spin splitting that arises from to the lower symmetric hexagonal structure, leading to comparably short spin relaxation times despite the expected small spin-orbit coupling effects. The cubic phase of GaN with its higher symmetry does not suffer from this extra contribution to the spin-splitting and shows thus longer spin relaxation times than, e.g., GaAs due to its smaller spin-splitting constant. The determination of Γ_e is, however, notoriously difficult, as is well known also from the thoroughly studied GaAs. Experimental values for Γ_e for cubic GaN are missing so far, but Γ_e can be calculated via the $k \cdot p$-formula[16]

$$\Gamma_e = \frac{1}{2} \frac{\alpha \hbar^3}{\sqrt{2 m^{*3} E_g}} \ ,$$

where the dimensionless constant α is given by

$$\alpha = \frac{4}{3} \frac{m^*}{m_{cv}} \eta (1 - \tfrac{1}{3}\eta)^{-1/2}$$

with $\eta = \Delta_{so}/(E_g + \Delta_{so})$. The constant m_{cv} can be approximated by $m_{cv} = m_e/\sqrt{3}$ with m_e as the free electron mass,[8,17] leading to $\Gamma_e = 0.13$ eVÅ^3 for[18,19] $E_g = 3.302$ eV, $\Delta_{so} = 0.017$ eV and $m^* = 0.13 m_e$. Full band structure calculations give, however, a considerably smaller value of $m_{cv} = 0.092 m_e$,[8] resulting in a value of $\Gamma_e = 0.84$ eVÅ^3, which is by more than a factor twenty smaller than in GaAs. Using $\Gamma_e = 0.84$ eVÅ^3, a spin relaxation time $\tau_s^{\text{theo}} = 565$ ps follows from Equation (2) for an estimated momentum scattering time $\tau_p = 100$ fs, giving good agreement with the experimental results [blue line in Figure 3(a)].

Sample B with its higher wurtzite phase content shows comparably long spin relaxation times than sample A [cf. Figure 1(a)]. The wurtzite phase content does therefore not seem to harm the long spin relaxation times, at least in the degenerate regime.

4. CONCLUSIONS

In conclusion, we demonstrated slow electron spin relaxation in bulk cubic GaN. The long spin relaxation times exceed 500 ps up to room-temperature, despite a very high n-type dopding of more than 10^{19} cm^{-3}, which results from the small spin-splitting constant in cubic GaN. The astonishingly weak temperature dependence of the spin relaxation is explained by Dyakonov-Perel theory for the highly degenerate regime.

5. ACKNOWLEDGMENTS

We gratefully acknowledge financial support by the German Science Foundation (DFG priority program 1285 'Semiconductor Spintronics' and DFG graduate program GRK 1464 'Micro- and Nanostructures in Optoelectronics and Photonics'), J. H. B. was supported by the Ruhr-University Research School funded by Germany's Excellence Initiative [DFG GSC 98/1].

REFERENCES

[1] Zutic, I., Fabian, J., and Sarma, S. D., "Spintronics: Fundamentals and applications," *Rev. Mod. Phys.* **76**, 323–410 (2004).

[2] Dietl, T., Ohno, H., Matsukura, F., Cibert, J., and Ferrand, D., "Zener Model Description of Ferromagnetism in Zinc-Blende Magnetic Semiconductors," *Science* **287**, 1019 (2000).

[3] Rudolph, J., Hägele, D., Gibbs, H. M., Khitrova, G., and Oestreich, M., "Laser threshold reduction in a spintronic device," *Appl. Phys. Lett.* **82**, 4516–4518 (2003).

[4] Nakamura, S. and Chichibu, S. F., eds., [*Introduction to Nitride Semiconductor Blue Lasers and Light Emitting Diodes*], CRC Press, Boca Raton (2000).

[5] Buß, J. H., Rudolph, J., Natali, F., Semond, F., and Hägele, D., "Temperature dependence of electron spin relaxation in bulk GaN," *Phys. Rev. B* **81**, 155216 (2010).

[6] Buß, J. H., Rudolph, J., Natali, F., Semond, F., and Hägele, D., "Anisotropic electron spin relaxation in bulk GaN," *Appl. Phys. Lett.* **95**, 192107 (2009).

[7] Krishnamurthy, S., van Schilfgaarde, M., and Newman, N., "Spin lifetimes of electrons injected into GaAs and GaN," *Appl. Phys. Lett.* **83**, 1761–1763 (2003).

[8] Yu, Z. G., Krishnamurthy, S., van Schilfgaarde, M., and Newman, N., "Spin relaxation of electrons and holes in zinc-blende semiconductors," *Phys. Rev. B* **71**, 245312 (2005).

[9] Dzhioev, R. I., Kavokin, K. V., Korenev, V. L., Lazarev, M. V., Meltser, B. Y., Stepanova, M. N., Zakharchenya, B. P., Gammon, D., and Katzer, D. S., "Low-temperature spin relaxation in n-type GaAs," *Phys. Rev. B* **66**, 245204 (2002).

[10] As, D. J., "Cubic group-III nitride-based nanostructures-basics and applications in optoelectronics," *Microelectron. J.* **40**, 204 (2009).

[11] Schupp, T., Lischka, K., and As, D. J., "MBE growth of atomically smooth non-polar cubic AlN," *J. Cryst. Growth* **312**, 1500–1504 (2010).

[12] D. J. As in *III-Nitride Semiconductor materials: Growth*, edited by M. O. Manasreh and I. T. Ferguson (Taylor and Francis, New York, 2003), ch. 9.

[13] Buß, J. H., Rudolph, J., Schupp, T., As, D. J., Lischka, K., and Hägele, D., "Long room-temperature electron spin lifetimes in highly doped cubic GaN," *Appl. Phys. Lett.* **97**, 062101 (2010).

[14] Dyakonov, M. I. and Perel, V. I., "Spin relaxation of conduction electrons in noncentrosymmetric semiconductors," *Sov. Phys. Solid State* **13**, 3023–3026 (1972).

[15] Dresselhaus, G., "Spin-Orbit Coupling Effects in Zinc Blende Structures," *Phys. Rev.* **100**, 580 (1955).

[16] Meier, F. and Zakharchenya, B. P., eds., [*Optical Orientation*], North-Holland, Amsterdam (1984).

[17] Song, P. H. and Kim, K. W., "Spin relaxation of conduction electrons in bulk III-V semiconductors," *Phys. Rev. B* **66**, 035207 (2002).

[18] Ramírez-Flores, G., Navarro-Contreras, H., Lastras-Martínez, A., Powell, R. C., and Greene, J. E., "Temperature-dependent optical band gap of the metastable zinc-blende structure β-GaN," *Phys. Rev. B* **50**, 8433 (1994).

[19] V. Bougrov and M. Levinshtein and S. Rumyantsev and A. Zubrilov in *Properties of Advanced Semiconductor Materials*, edited by M. E. Levinshtein, S. L. Rumyantsev, and M. S. Shur (Wiley, New York, 2001), ch.1.